E3S Web of Conferences **362**, 02002 (2022)
BuildSim Nordic 2022
https://doi.org/10.1051/e3sconf/202236202002

Performance analysis of a solar thermal system coupled with a ground source heat pump in Nordic conditions

Sandra Fransson Wilberg *, Habtamu Bayera Madessa , Arnab Chaudhuri
Department of Civil Engineering and Energy Technologi
OsloMet - Oslo Metropolitan University
Oslo, Norway
*Correspoing author: sandra.wilberg@hotmail.com

Abstract

The main objective of this work is to investigate the energy and exergy performance of a solar assisted ground source heat pump for a school building designed according to Norwegian passive house standard. The system is designed in such a way that the solar collector prioritizes to provide heat to the hot water tank and whenever there is excess heat from the solar collector it can be used to charge the ground borehole. A detailed thermodynamic analysis of the system has been carried out in Engineering Equation Solver (EES). Isobutane (R600a), propane (R290), ammonia (R717) and solstice (R1234ze(E)) have been investigated as working fluid for the heat pump. The result revealed that the solar collector and the different working media have affected both the COP and the exergy of the system. Moreover, the mass flow rate of the brine and the length of the borehole affect the performance of the system.

Introduction

The building sector's energy demand has been rising the last decades and it is now accounting for 30% of the global final energy consumption, making it one of the largest energy consumption sectors (Berardi (2015)). The Paris agreement is adopted by 196 countries in 2016 (UNFCCC (2015)), and the UN climate report is expressing a deep concern for the environment (Masson-Delmotte et al. (2021)), and it has heightened the focus on reducing energy usage. It is, therefore, vital to improve the performance of energy systems in buildings and minimize their greenhouse gas emissions to meet the Paris agreement's target of limiting global warming to 1.5 °C compared to the prediction.

As more passive houses and low-energy buildings have been built in recent years, the need for efficient energy systems has grown. As well, due to the change in weather pattern and cold climate in the north, there is still some uncertainty about how some types of energy sources can best be utilized for the building sector, like solar systems. Ground source heat pumps (GSHP) are a well-established technology in Norway today. Solar energy is, however, less used, particularly solar thermal energy systems. Nonetheless, there has been an increase in interest in combining these two technologies to improve the heat pump operating conditions and minimize the need of an auxiliary heating unit. Hwang et al. (2021), Razavi et al. (2018) and Girard et al. (2015) have compared the performance of the solar assisted ground source heat pump (SGSHP) to a conventional GSHP, and the results showed that the benefits of having solar thermal energy combined with GSHP. The configurations of SGSHP can be done in a variety of ways. The heat generated by the solar collectors can be utilized to raise the evaporation temperature, recharge the ground, or used to produce the building's domestic hot water, or a combination of these methods. In recent years, there has been an increase in the number of published research works examining how system solutions for SGSHP affects performance, and Reda and Laitinen (2015) and Yang et al. (2015) reported different positive outcomes from each configuration studied.

The main objective of this paper is to investigate the energy and exergy performance of a SGSHP for a school building designed according to the Norwegian passive house standard, (NS3701 (2012)). The energy system will provide energy to a hot water storage tank providing domestic hot water (DHW) and space heating. The system designed in such a way that flat plate solar collectors prioritize providing heat to the hot water storage tank and whenever there is excess heat from the solar collector, it can be used to charge the ground borehole. A detailed thermodynamic analysis of the selected system has been carried out in Engineering Equation Solver (EES) (Software (2021)), and the potential working fluids isobutane (R600a), propane (R290), ammonia (R717), and solstice (R1234ze(E)) have been investigated. Moreover, sensitivity analyses have been conducted to identify how different parameters influence the system's performance and provide important knowledge for system optimization.

Method

Case setup

The chosen solution for this work is illustrated in figure 1. The solar collector is used to heat the water tank and recharge the ground. The circulation pump before the SC will start when the surface temperature of the SC is 10°C or higher. Below this temperature, the SC will not be able

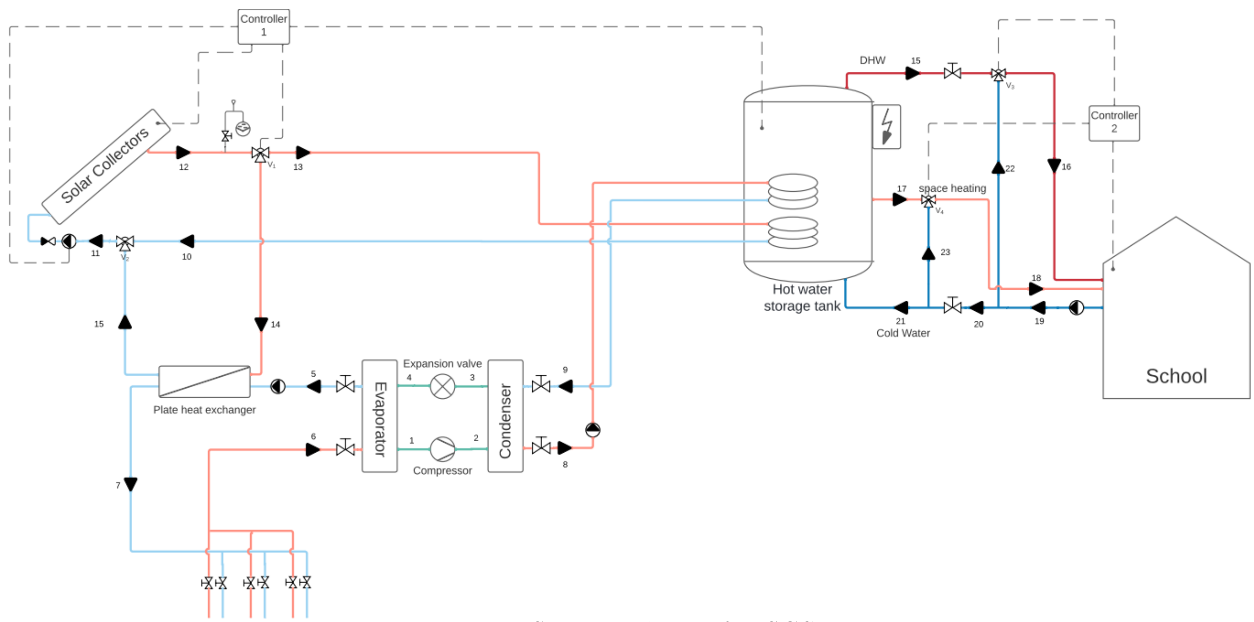

Figure 1: System solution for SGSHP

to provide significant temperature rise in the water tank or heat exchanger, as mentioned by Sørensen (2017). If the temperature in the SC is 5K greater than the water tank temperature, the controller will direct the working fluid through the valve V_1 to the water tank. If this isn't the case, the controller will send the working fluid to the plate heat exchanger, which will heat the brine from the HP and to the ground heat exchanger (GHX). When the SC is unable to heat the water tank to 70 °C alone, the HP will start, and begin extracting heat from the GHX. If neither the GSHP nor the SC can maintain the set point in the tank, an electrical heater will be activated. Which scenario the SC should work is determined by a controller which examines and compares the temperature at specified places and based on this adjust the flow through valve V_1.

The hot water storage tank is split into three sections. The SC heats the low-temperature water at the bottom, where the cold water enters. In the middle, the HP connected to the heat exchanger (HX) heats the tank further and the space heating is extracted. The electrical heater is placed on the top section as an auxiliary unit, which will turn on when the water temperature falls below the set point. The DHW will also be distributed to the building from the top section. This is beneficial for the SC's efficiency, which is better at low temperatures, and it ensures that it doesn't compete with the electric energy.

The SGSHP system is dimensioned and analyzed based on a reference school building located in Oslo with a usefull area of 900 m^2, where the mean air temperature is 6.3 °C and the designed outdoor air temperature during the winter is – 19.8°C, (byggforsk (2018)). The building is classified as a passive house and should therefor satisfy Criteria for passive houses and low energy buildings, (NS3701 (2012)).

According to SN-NSPEK3031 (2021), the set point for heating the school building is 21°C. As a result, ΔT in the energy calculation will be $21 - (-19.8) = 40.8$ °C, which gives an energy and power demand of the building 23 670 $kWh/year$ and 26 626 $W/year$, respectively.
The SC is dimensioned to cover 60% of the DHW demand, 2700 $kWh/year$. The working fluid inside the solar system is Ethylene-Glycol mixture with a concentration of 35%.
The ground heat exchanger is made of single U-tube collectors, high-density polyethylene with a thermal conductivity of 0.35 W/mK, connected in parallel. The depth of the boreholes is selected to be 130 meters with an internal diameter of 0.1 meters.
In order to reduce the number of on-off time for the operation of a HP and improve its performance, a HP should be sized for 50-60% of the maximum building heating rate demand and 80-95 percent of the energy demand, according to Zijdemans (2014). The HP in this study will therefore be dimensioned for 55% of the total power demand and 90% of the total power demand. The heat pump is dimensioned for 15 kW.

Solar collector

The thermal efficiency of the SC expresses the useful energy gain over the incident solar energy, and can be obtained from equation 1 (CEN-EN12975-1 (2006)).

$$\eta_{SC} = \eta_0 - \frac{a_1(T_m - T_a)}{G} - \frac{a_2(T_m - T_a)^2}{G} \quad (1)$$

η_0, a_1 and a_2 is information given by the solar collector manufacturer, THERMIQUE (2017).

For the exergy analysis of the solar collector system, the general exergy balance from equation 2 is employed.

$$\Sigma X_{des} = \Sigma X_{in} - \Sigma X_{out} - \Sigma X_s \quad (2)$$

Since the system is under steady-state conditions, the stored exergy $\Sigma X_s = 0$. According to García-Menéndez et al. (2022), exergy into a solar system is separated into two parts: the working fluid and the solar radiation, and the following formulae are used to compute them.

$$X_{in,f} = m_{SC} c_{p,SC,f} (T_{11} - T_a - T_a \ln \frac{T_{11}}{T_a}) \quad (3)$$

$$X_{in,sr} = Q_i (1 - \frac{4}{3} \frac{T_a}{T_{sun}} + \frac{1}{3} (\frac{T_a}{T_{sun}})^4) \quad (4)$$

The exergy out of the system is only from the working fluid.

$$X_{out,f} = m_{SC} c_{p,sun} (T_{12} - T_a - T_a \ln \frac{T_{12}}{T_a}) \quad (5)$$

The second law efficiency is calculated using the following equation.

$$\eta_{II,sun} = \frac{X_{out,f} - X_{in,f}}{X_{in,f}} \quad (6)$$

Ground heat exchanger

Assuming that the pipe heat loss between the borehole and evaporator is negligible, the heat extracted from the borehole field is equal to the heat transfer to the working fluid in the evaporator.

$$Q_{Ground} = Q_{evap} \quad (7)$$

$$Q_{ground} = Q_{ghx} N_{boreholes} \quad (8)$$

The heat extracted from each borehole is determined by the following equations.

$$q_{ghx} = \frac{\Delta T}{R_{tot}} \quad (9)$$

$$Q_{ghx} = q_{ghx} L_{pipe,ghx} \quad (10)$$

ΔT represents the temperature difference between the soil and the brine temperature.

$$R_{tot} = R_{grout} + R_{pipe} + R_{brine} \quad (11)$$

Where $\mathrm{R}_{grout} = \frac{\ln \frac{D_b}{D_{ed,o}}}{2\pi k_g}$, $R_{pipe} = \frac{\ln \frac{D_{ed,o}}{D_{ed,i}}}{2\pi k_p}$ and $\mathrm{R}_{brine} = \frac{1}{\pi D_{ed,i} h_{brine}}$

The exergy and second law efficiency formula utilized for the SC were also employed in the exergy analysis of the GHX (García-Menéndez et al. (2022)).

$$X_{i,ghx} = m_{brine} c_{p,ghx} (T_7 - T_g - T_g \ln \frac{T_7}{T_g}) \quad (12)$$

$$X_{o,ghx} = m_{brine} c_{p,ghx} (T_6 - T_g - T_g \ln \frac{T_6}{T_g}) \quad (13)$$

$$\eta_{II,ghx} = \frac{X_{o,ghx}}{X_{i,ghx}} \quad (14)$$

The exergy destruction for the whole borehole field was determined.

$$X_{des,ghx} = m_{brine} (\psi_7 - \psi_6) + Q_{ground} (1 - \frac{T_0}{T_g}) \quad (15)$$

Heat pump

The COP of the HP is calculated using equation 16.

$$COP_{HP} = \frac{Q_{cond}}{W_{comp}} \quad (16)$$

Where the work done on the compressor, W_{comp}, is calculated by equation 17.

$$W_{comp} = m_{refg} (h_{2a} - h_1) \quad (17)$$

The second law of efficiency for the different components of the HP is calculated are follows.

$$\eta_{II,comp} = 1 - \frac{X_{des,comp}}{W_{comp}} \quad (18)$$

$$\eta_{II,cond} = 1 - \frac{X_{des,cond}}{m_{refg} (\psi_2 - \psi_3)} \quad (19)$$

$$\eta_{II,exp} = 0 \quad (20)$$

$$\eta_{II,evap} = 1 - \frac{X_{des,evap}}{m_{refg} (\psi_4 - \psi_1)} \quad (21)$$

The exergy flow due to mass transfer, when the kinetic and potential energy is neglected, is calculated by the following equation.

$$(\psi_i - \psi_e) = (h_i - h_e) - T_0 (s_i - s_e) \quad (22)$$

The exergy destruction is calculated by the following equations for the different components of the HP.

$$X_{des,comp} = T_0 m_{refg} (s_2 - s_1) \quad (23)$$

$$X_{des,cond} = T_0 m_{refg} (s_3 - s_2) + \frac{Q_{cond}}{T_{m,water}} \quad (24)$$

$$X_{des,exp} = T_0 m_{refg} (s_2 - s_1) \quad (25)$$

$$X_{des,evap} = T_0 m_{refg} (s_1 - s_4) - \frac{Q_{evap}}{T_{m,brine}} \quad (26)$$

Since the HP is placed inside the school building, the dead state temperature, T_0, is set to 21°C.

The input data for the mathematical models is listed in table 1

Table 1: Input data for the mathematical models.

Parameter	Value
Ambient air temperature, T_a	286 K
Dead state temperature, T_0	279.3 K
Solar irradiance, G	800 W/m^2
Surface temperature of the sun, T_{sun}	4 333 K
Mass flow, m_{SC}	0.04 kg/s
Grout material	Water
Number of tubes, N_{tube}	2
Pipe outer diameter, $D_{pipe,o}$	0.04 m
Soil temperature, T_s	283.3 K
Brine temperature out of the HP, T_5	275 K
Mass flow rate, m_{GHX}	0.5 kg/s
Exit temperature of the refrigerant at state point 1, T_1	275 K
Exit temperature of the refrigerant at state point 3, T_3	318 K
Exit temperature of the refrigerant at state point 4, T_4	270 K
Pipe diameter of HP, D_{HP}	0.003 m

Validation of the models

The developed thermodynamics models were verified against other models to check the level of their accuracy. Using input data from the published articles, the findings were compared and evaluated, as shown in table 2.

*Table 2: Validation of the mathematical model. *Guarracino et al. (2019)**Madessa et al. (2017)***Esen et al. (2007)*

Value	This study	Models used for validation	Devation
η_{th}	42%	41%*	2.4%
T_6	7.6-3.8°C	7.4-4.4°C **	10.6%
η_i	68%	70% ***	2.9%
COP	2.88	2.5-2.77 ***	3.8%

The small deviations for all the parameters presented in the table ensure the quality of the mathematical model and emphasizing the accuracy of the calculations used in this work. The highest deviation came from comparing how the mass flow rate in the borehole influence the temperature out of the GHX, T_6. The obtained temperatures from this paper is lower than the validation model, and decreases more rapidly with the increase of the mass flow. This is maybe due to the of the use of equivalent diameter in this work. Moreover, the exact soil temperature is not mentioned in Madessa et al's study, and this can also contribute to differences.

Results and discussions

Solar collector

The thermal efficiency of a solar collector is used to assess its performance. For the chosen type of SC, ambient temperature at 293 K and solar irradiance at 800 W/m^2, the thermal efficiency of the solar collectors was found to be 58%. This corresponds to the information given by DieTrich THERMIQUE (2017) for their flat plate solar collectors, emphasizing the accuracy of this calculation. As it can be seen from equation 1, the ambient temperature and solar flux, which can fluctuate greatly during the day, have an impact on the efficiency of the collector as shown in figure 2.

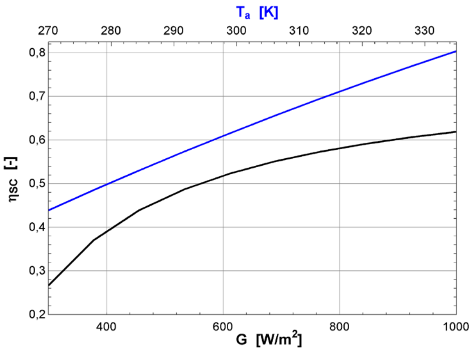

Figure 2: Variation in thermal efficiency with varying solar flux and ambient temperature

The exergy into and out of the SC was calculated for the chosen temperature and solar irradiance conditions, and was found to be 4282.9 W and 1309 W respectively. The corresponding second order efficiency of the solar collector was also found to be 33.44 %. Figure 3 shows how the inlet temperature effect this efficiency.

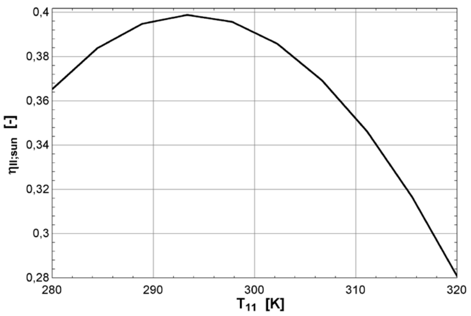

Figure 3: The impact of the inlet temperature of the SC on the second order efficiency

The variation in the fluid inlet temperature to the SC reveals that the exergy efficiency increases up to 294 K and then decreases as the inlet temperature rises further. This indicates that keeping a inlet temperature close to the ambient temperature will reduce the heat loss to the surrounding and a lower inlet temperature is therefor generally preferable for the SC.

Ground heat exchanger

The depth and the number of the boreholes are critical to investigate in order to achieve optimal operation of the HP. The optimal relation between the length of each borehole and the number of boreholes depends on several parameters, such as the types of grout materials. Figure 4 illustrates the effect of three different grout materials: water, cement and Bentionite mixture, on the number of boreholes for a fixed mass flow rate of 0.5 kg/s when the depth of the borehole varies between a normal range. The water used as grout is considered to be stagnant, and the effect of the convection heat transfer is ignored.

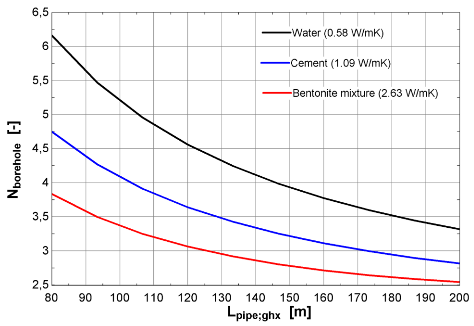

Figure 4: Relation between the depth and number of boreholes to achieve the energy demand with different types of grout

As shown in figure 4, since water has the lowest thermal conductivity, the number of boreholes required for this grout material is greater than those required for the other two grout materials. The bentonite mixture has a thermal conductivity of 2.63 W/mK, and when it replaces the water with this mixture the length of a borehole can be reduced by 35%, which means reduction in both investment and operation cost of the system, and as well it might reduce the heat exchange between the boreholes under operation.

Another parameter influencing the relation between the depth and number of boreholes is the mass flow rate of the brine in each of the boreholes. In figure 5, three different flow rates were analyzed.

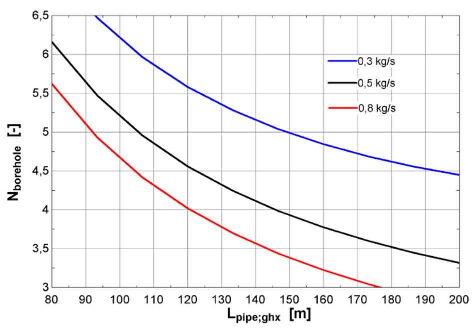

Figure 5: Relation between the depth and number of boreholes to achieve the energy demand with different mass flow rates

The results shows an increase in the mass flow rate reduce either the number of boreholes or the borehole length, which affects again both the investment and operation cost.

Figure 6 shows how the rate of exergy destruction in the borehole field is affected by inlet and outlet temperature of brine to/from the borehole.

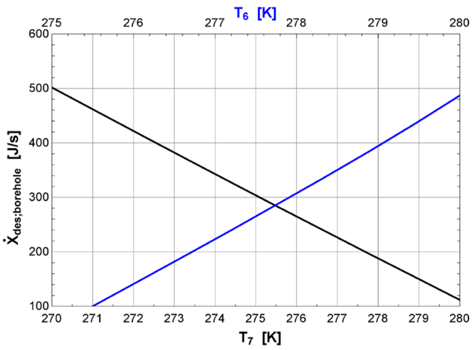

Figure 6: The influence the inlet and outlet temperature on the exergy destruction of the borehole

As the inlet temperature rises, the exergy destruction decreases, while the exergy destruction increases with increase in the outlet temperature. As a result, to achieve lesser exergy destruction, the minimal temperature difference between the outlet and inlet is preferred. This underlines a positive outcome from using HX connected to the SC to heat up the boreholes, instead of implementing longer boreholes to achieve the needed temperature in to the HP.

The DHW demand may be lower in the summer, and the SC can be able to charge the boreholes. Throughout this time, the SC can replenish the ground more effectively. This will help to reduce ground depletion in the long run.

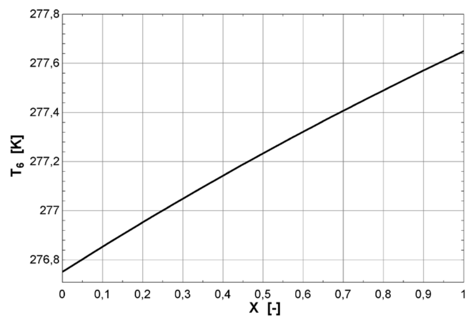

Figure 7: effect of the excess energy from the SC on the outlet temperature of the brine from the borehole

Figure 7 illustrates how the variation of the portion of the mass flow rate sent down to the HX affects the outlet temperature of the boreholes. When X is equal to 1, all of the mass flow rate in the solar circuit is directed to the HX. The figure shows that when the heat exchanger receives more heat from the SC, the outlet temperature of the borehole increases, and this help to rise the exit temperature of the borehole. Therefor, increasing the inlet temperature through the heat exchanger is a good option to reduce the exergy destruction in the borehole and helps to get the right temperature in to the evaporator.

Heat pump

In order to investigate the performance of the working fluids, COP of the HP was calculated for each refrigerant according to equation 19. The results show that the COP for R600a, R290, R717, and R1234ze(E) were 4.04, 4.13, 4.39, and 3.89, respectively, when the heat transfer in the condenser was set at 15 kW and the length of each borehole was 130 meters. Figure 8 illustrates how the mass flow rate of the refrigerant effects the COP.

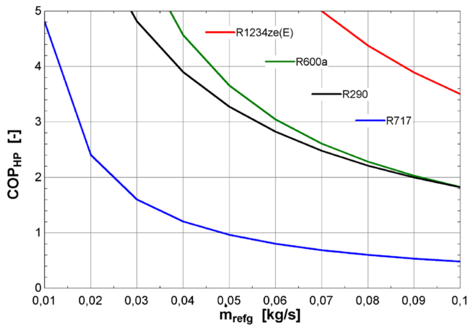

Figure 8: The COP of the HP with the different refrigerant when the mass flow rate is altered and the length of the borehole is set to 130 m.

The exergy destruction for the four components of the HP is presented in table 3.

Table 3: Calculated exergy destruction in each component of the HP for the different refrigerants

Component	R600a	R290	R717	R1234-ze(E)
Evaporator $[W]$	259.0	260.9	267.8	245.0
Compressor $[W]$	1057.0	835.9	635,6	1140.0
Condenser $[W]$	243.3	273	599,5	252.5
Expansion valve $[W]$	504.4	607.7	245,3	577.0
Sum	2064.0	1978.0	1748.0	2215.0

R600a and R290 have the nearly the similar performance. This could be due to the fact that these two have nearly similar thermophysical properties. The R1234ze(E) HP generates the most exergy destruction, while R717 generates the least. The results also show that the compressor incurs the most significant exergy destruction, and stands for over 35% of the total exergy destruction. Figure 9 illustrates how subcooling of the refrigerant reduces the exergy destruction of the HP.

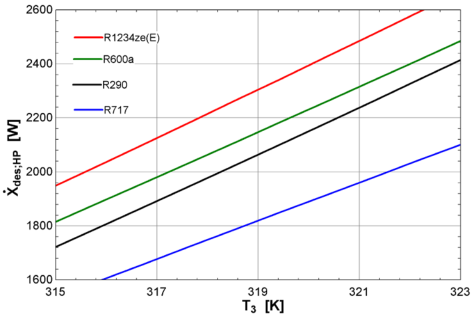

Figure 9: The total exergy destruction in the HP with variation in the outlet temperature of the condenser for each refrigerant.

Subcooling the refrigerants after the condenser has given positive result on the exergy destruction of the HP, and is thus a strategy to implement in order to minimize the HP's total exergy destruction and the second order efficiency. In this study, the temperature out of the condenser is subcooled by 5K, and if this had not been done, the total exergy destruction would be increased by 17%.

Conclusion

The main purpose of this work was to investigate the performance of SGSHP for school building designed according to Norwegian passive house standard. EES was used to study the energy and exergy of the system.

When the SC produces excess heat, it can be directed to charge the borehole. This helps preventing thermal imbalance of the soil over time and increasing the borehole's outlet temperature. The inlet temperature of the SC has a substantial impact on the second order efficiency of the SC, and with a cold climate like Norway has, it is very important to keep a low inlet temperature to minimize the heat loss to the surroundings.

For the borehole field, the optimal relation between the number of boreholes and length depend on the type of the grout material. The study shows, choosing a grout with high thermal conductivity is favorable in order to reduce the depth and number of boreholes, which is cost-beneficial.

R717 as a working fluid was found to achieve the best overall performance for the HP under the specified conditions, having the highest COP at 4.39 and lowest exergy destruction. The compressor stand for a significant part of the HP's exergy destruction, and it was discovered that subcooling the refrigerant after the condenser might reduce exergy destruction and improves the HP's overall performance.

In summary, SGSHP appear to be a well-suited energy system for heating a passiv house school building in Norway under the conditions studied. Assumptions and simplifications have been made through the study, thus it's treated with caution.

Nomenclature

Greek letters	Description
η_{th}	Thermal efficiency [-]
η_0	Optical efficiency [-]
$\eta_{II,SC}$	Second order efficiency-SC [-]
$\eta_{II,comp}$	Second order efficiency compressor [-]
$\eta_{II,cond}$	Second order efficiency condenser [-]
$\eta_{II,evap}$	Second order efficiency evaporator [-]
$\eta_{II,exp}$	Second order efficiency expansion valve [-]
ψ_1	Flow specific exergy at point 1 [kJ/kg]
ψ_2	Flow specific exergy at point 2 [kJ/kg]
ψ_3	Flow specific exergy at point 3 [kJ/kg]
ψ_4	Flow specific exergy at point 4 [kJ/kg]
Δ	Interval [-]

Abbreviation	Explanation
COP	Coefficient of performance
DHW	Domestic hot water
EES	Engineering equation solver
GHX	Ground heat exchanger
GSHP	Ground source heat pump
GWP	Global warming potential
HP	Heat pump
HX	Heat exchanger
SC	Solar collector
SGSHP	Solar assisted ground source heat pump

Symbols	Description
A	Area [m^2]
a_1	1st order heat loss coefficient [W/m^2K]
a_2	2nd order heat loss coefficient [W/m^2K^2]
$c_{p,SC,f}$	Heat capacity-working fluid in the SC [J/kgK]
$c_{p,ghx}$	Heat capacity of the brine [J/kgK]
D_b	diameter of the borehole [m]
$D_{ed,i}$	Equivalent inner diameter-borehole pipe [m]
$D_{ed,0}$	Equivalent outer diameter-borehole pipe [m]
G	Solar irradiance [W/m^2]
h_{brine}	Heat transfer coefficient-brine [W/m^2K]
h_1	Specific enthalpy at point 1 [J/kg]
h_{2a}	Specific enthalpy before the condenser [J/kg]
k_g	Thermal conductivity-grout [W/mK]
k_p	Thermal conductivity-borehole pipe [W/mK]
$L_{pipe,ghx}$	Length of the pipe in one borehole [m]
m_{brine}	Mass flow rate-brine [kg/s]
m_{SC}	Mass flow rate-SC working fluid [kg/s]
m_{refg}	Mass flow rate-refrigerant [kg/s]
$N_{boreholes}$	Number of boreholes [W]
Q_{cond}	Heat extraced in the condenser [W]
Q_{evap}	Heat extraced in the evaporator [W]
Q_{ground}	Heat extraced from the borehole field [W]
Q_i	Energy in to the solar system from the sun [W]
Q_{GHX}	Heat extraced from one boerhole [W]
q_{GHX}	Heat extraced from the borehole per meter [W/m]
R_{brine}	Thermal resistance-brine [mK/W]
R_{grout}	Thermal resistance-grout [mK/W]
R_{pipe}	Thermal resistance-pipe [mK/W]
s_1	Specif entropy at point 1 [J/kgK]
s_2	Specif entropy at point 2 [J/kgK]
s_3	Specif entropy at point 3 [J/kgK]
s_4	Specif entropy at point 4 [J/kgK]
T_a	Ambient temperature [K]
T_m	Mean temperature of the SC [K]
$T_{m,water}$	Mean temperature of the water in the condenser [K]
T_s	Mean temperature of the soil [K]
T_{sun}	Surface temperature of the sun [K]
T_0	Dead state temperature of the system [K]
T_6	Outlet temperature of the GHX [K]
T_7	Inlet temperature of the GHX [K]
T_{11}	Inlet temperature of the solar collector [K]
T_{12}	Outlet temperature of the solar collector [K]
U	Overall heat transfer coefficient [W/m^2K]
W_{comp}	Work in to the compressor [W]
$X_{des,comp}$	Exergy destruction-compressor [W]
$X_{des,cond}$	Exergy destruction-condenser [W]
$X_{des,evap}$	Exergy destruction-evaporator [W]
$X_{des,exp}$	Exergy destruction-expansion valve [W]
$X_{des,ghx}$	Exergy destruction-borehole field [W]
X_{in}	Exergy in to the system [W]
$X_{in,f}$	Exergy of the fluid in the inlet of the SC [W]
$X_{in,sr}$	Exergy due to the solar irradiance [W]
X_{in}	Exergy out of the system [W]
$X_{out,f}$	Exergy of the fluid in the outlet of the SC [W]

https://doi.org/10.1051/e3sconf/202236202002

References

Berardi, U. (2015). Building energy consumption in us, eu, and bric countries.

byggforsk, S. (2018). 451.021 klimadata for termisk dimensjonering og frostsikring.

CEN-EN12975-1 (2006). Thermal solar systems and components - solar collectors part 1: General requirements.

Esen, H., M. Inalli, M. Esen, and K. Pihtili (2007). Energy and exergy analysis of a ground-coupled heat pump system with two horizontal ground heat exchangers.

García-Menéndez, D., J. C. Ríos-Fernández, A. M. Blanco-Marigorta, and M. J. Suárez-López (2022). Dynamic simulation and exergetic analysis of a solar thermal collector installation.

Girard, A., E. J. Gago, T. Muneer, and G. Caceres (2015). Higher ground source heat pump cop in a residential building through the use of solar thermal collectors.

Guarracino, I., J. Freeman, A. Ramos, S. A. Kalogirou, N. J. Ekins-Daukes, and C. N. Markides (2019). Systematic testing of hybrid pv-thermal (pvt) solar collectors in steady-state and dynamic outdoor conditions.

Hwang, J., D. Song, and T. Lee (2021). The effect of coupling solar thermal system and geothermal heat pump systems in areas with unbalanced heating and cooling demand.

Madessa, H. B., T. B, P. F. Bye, and E. A (2017). Parametric study of a vertically configured ground source heat pump system.

(2021). *Climate Change 2021: The Physical Science Basis. Contribution of Working Group I to the Sixth Assessment Report of the Intergovernmental Panel on Climate Change*.

NS3701 (2012). Criteria for passive houses and low energy buildings - non-residential buildings.

Razavi, S. H., R. Ahmadi, and A. Zahedi (2018). Modeling, simulation and dynamic control of solar assisted ground source heat pump to provide heating load and dhw.

Reda, F. and A. Laitinen (2015). Different strategies for long term performance of sagshp to match residential energy requirements in a cold climate.

SN-NSPEK3031 (2021). Energy performance og buildings- calculation of energy needs and energy supply.

Software, F.-C. (2021). Engineering equation solver.

Sørensen, Å. L., T. C. B. . N. H. K. (2017). Solvarme i kombinasjon med andre varmekilder. norsk solenergiforening.

THERMIQUE, D. D. (2017). Solar installations - solar collectors, tanks and systems for individual and collective installations.

UNFCCC (2015). The paris agreement.

Yang, W., L. Sun, and Y. Sun (2015). Experimental investigations of the performance of a solar-ground source heat pump system operated in heating modes.

Zijdemans, D. (2014). *Vannbaserte oppvarmings-og kjølesystemer*.